Comments and Corrections to "Capacity of Multiple-Antenna Systems With Both Receiver and Transmitter Channel State Information"

Kamal Singh and Chandradeep Singh

***Abstract*— The correspondence cited in the above article derived ergodic capacity of the coherent multiple-input multiple-output (MIMO) channel in independent and identically distributed (IID) Rayleigh fading. While the theoretical results are correct, several plots in the paper are incorrect. In this correspondence, we correct the plots. More importantly, the corrected plots present an interesting and compelling contrast between performances of the coherent MIMO systems with and without channel state information at the transmitter; whereas this view is somewhat limited in the above article because of flaws in the capacity curves.**

***Index Terms*— Ergodic capacity, multiple-input multiple-output (MIMO), Rayleigh fading channel, power control, channel state information at the transmitter (CSIT).**

I. Introduction

THE main objective of this note is to correct the ergodic capacity versus SNR graphs of the MIMO fading channel in [1]. The ergodic capacity of a coherent MIMO fading channel $\boldsymbol{H}$[1] with perfect instantaneous channel state information H at the transmitter (CSIT) can be obtained by solving the following problem[2] [2, Section 8.2]:

$$\max_{Q(H):\mathrm{Tr}(\mathbb{E}_{\boldsymbol{H}}[Q(\boldsymbol{H})])\le P} \mathbb{E}_{\boldsymbol{H}}[\log\det(\boldsymbol{I}_{N_R}+\boldsymbol{H}Q(\boldsymbol{H})\boldsymbol{H}^{\dagger})] \quad (1)$$

where $Q(H)$ is the input covariance matrix and P is an average power constraint at the transmitter, which implies $\mathrm{Tr}(\mathbb{E}_{\boldsymbol{H}}[Q(\boldsymbol{H})]) \le P$. In [1], the authors solved the optimization in (1) for the IID Rayleigh fading model, i.e. channel matrix $\boldsymbol{H}$ has i.i.d. entries and each entry in $\boldsymbol{H} \sim \mathcal{CN}(0,1)$, to yield the capacity with CSIT as

$$C = m\,\mathbb{E}_{\boldsymbol{\lambda}}\big[\log(1+\boldsymbol{\lambda}P(\boldsymbol{\lambda}))\big] \quad (2)$$

where $m = \min(N_R, N_T)$ and the optimal *waterfilling* power scheme $P(\lambda) = (1/\lambda_0 - 1/\lambda)^+$. We will use explicit notation $C(x,y,z)$ (resp. $\widehat{C}(x,y,z)$) to denote the capacity of this $x \times y$ MIMO fading channel with CSIT (resp. without CSIT) under constraint z on the average transmit power. Precisely, the ergodic capacity has an integral-form expression as given in Eq. (58) in [1], and is reproduced here with a simple change of variables[3] as follows:

$$C(N_R, N_T, P) = m\int_{\lambda_0}^{\infty} \log\left(\frac{\lambda}{\lambda_0}\right) f_{\boldsymbol{\lambda}}(\lambda)d\lambda \quad (3)$$

where λ_0 is the threshold parameter determined from

$$\int_{\lambda_0}^{\infty}\left(\frac{1}{\lambda_0}-\frac{1}{\lambda}\right) f_{\boldsymbol{\lambda}}(\lambda)d\lambda = \frac{P}{m} \quad (4)$$

and the eigenmode distribution $f_{\boldsymbol{\lambda}}(\lambda)$ is given by

$$f_{\boldsymbol{\lambda}}(\lambda) = \frac{e^{-\lambda}\lambda^{n-m}}{m}\sum_{k=0}^{m-1}\frac{k!}{(k+n-m)!}[L_k^{n-m}(\lambda)]^2 \quad (5)$$

where, in turn, $n = \max(N_R, N_T)$ and $L_k^{n-m}(\lambda)$, the associated Laguerre polynomial of order k, has a closed-form expression given as

$$L_k^{n-m}(\lambda) = \sum_{p=0}^{k}\frac{(-\lambda)^p}{p!}\binom{k+n-m}{k-p}. \quad (6)$$

The ergodic capacity of this coherent MIMO channel *without* CSIT is given by

$$\widehat{C}(N_R, N_T, P) = m\int_0^{\infty}\log(1+\lambda P/N_T)\, f_{\boldsymbol{\lambda}}(\lambda)d\lambda \quad (7)$$

and the optimal power allocation is obtained by dividing the total transmit power P equally among all transmit antennas [3, Theorem 2]. It is easy to verify that

$$C(N_R, N_T, P) = C(N_T, N_R, P), \quad (8)$$

and

$$\widehat{C}(N_R, N_T, P) \ne \widehat{C}(N_T, N_R, P) \quad (9)$$

holds in general, except with equality when $N_R = N_T$. In fact, it is easy to check that for $N_R > N_T$,

$$\widehat{C}(N_R, N_T, P) > \widehat{C}(N_T, N_R, P) \text{ holds.} \quad (10)$$

In the following, for simplicity of notation, we will drop the functional dependence so that C and $\widehat{C}$ should be understood

Manuscript received December 24, 2019; revised December 28, 2020; accepted May 3, 2021. Date of publication June 2, 2021; date of current version July 14, 2021. *(Corresponding author: Kamal Singh.)*

Kamal Singh was with the Department of Electrical Engineering, IIT Bombay, Mumbai 400076, India. He is now with the Department of Electrical Engineering, Shiv Nadar University, Greater Noida 201314, India (e-mail: kamal.singh@snu.edu.in).

Chandradeep Singh was with the Department of Electrical Engineering, IIT Bombay, Mumbai 400076, India. He is now with the Department of Electrical Engineering, National Cheng Kung University, Tainan 701, Taiwan (e-mail: chandradeep.chd@gmail.com).

Communicated by A. Eckford, Associate Editor for the IEEE Transactions on Information Theory.

Digital Object Identifier 10.1109/TIT.2021.3085248

[1]The matrix $\boldsymbol{H}$ is a $N_R \times N_T$ matrix, where N_R and N_T indicate the number of receive and transmit antennas, respectively.

[2]Covariance matrix of the receiver AWGN noise vector, generally denoted as $N_0\boldsymbol{I}_{N_R}$ in the literature, is taken to be the identity i.e. $N_0 = 1$.

[3]The γ variable in Eq. (58) in [1] and λ variable in Eq. (3) above are related as $\gamma = \lambda\frac{P}{mN_0}$.

TABLE I

$N_R = 4$, $N_T = 4$

SNR (dB)	Capacity (Monte Carlo) (bits/s/Hz)	Capacity (Numerical) (bits/s/Hz)
-15	1.182976	1.182924
-10	2.518979	2.519749
-5	4.788550	4.789042
0	8.141317	8.141885
5	12.502087	12.506322
10	17.699588	17.695610

TABLE II

$N_R = 4$, $N_T = 6$

SNR (dB)	Capacity (Monte Carlo) (bits/s/Hz)	Capacity (Numerical) (bits/s/Hz)
-15	1.461202	1.461242
-10	3.108600	3.108137
-5	5.894179	5.894378
0	9.973844	9.974640
5	15.256107	15.255904
10	21.346760	21.346403

TABLE III

$N_R = 4$, $N_T = 8$

SNR (dB)	Capacity (Monte Carlo) (bits/s/Hz)	Capacity (Numerical) (bits/s/Hz)
-15	1.714074	1.714015
-10	3.633365	3.634128
-5	6.858986	6.859198
0	11.528260	11.527121
5	17.324821	17.326976
10	23.673975	23.674296

to refer to $C(N_R, N_T, P)$ and $\widehat{C}(N_R, N_T, P)$ respectively. In the next section, we present counter ergodic capacity results with detailed justifications followed by comparison with the existing curves in the correspondence cited in the title. Corrections are also applied to the plots for the cut-off and the outage probability bounds in [1]. The note concludes with a brief discussion and implication of the corrected capacity plots with and without CSIT.

II. Counter Results

The focus is on the ergodic capacity versus SNR curves for the MIMO Rayleigh channel with CSIT presented in Fig. 5 (or Fig. 6) in [1]. In this section, we present counter results for the ergodic capacity of the MIMO Rayleigh channel with CSIT computed using two independent approaches: *one* set of results is computed using standard root-finding algorithms to evaluate the waterfilling level $1/\lambda_0$ in Eq. (4) and then using numerical integration in Eq. (3), and the *second* set of results using Monte Carlo simulation.[4] The range of SNR,[5] N_T and N_R are chosen as identical to that in [1]. The computed values with these two methods are close and thus, suggesting the correctness of the results; precisely, the values match exactly up to 2 decimal places, see Table I-Table V.

The capacity values with CSIT in Table I-Table V are plotted in Figs. 1 and 2 along with the corresponding capacity values *without* CSIT. The capacity results without CSIT are determined by solving the integral in (7) numerically and are also verified with Monte Carlo simulations, see Table VI-Table XIV in Appendix A.

TABLE IV

$N_R = 4$, $N_T = 10$

SNR (dB)	Capacity (Monte Carlo) (bits/s/Hz)	Capacity (Numerical) (bits/s/Hz)
-15	1.949946	1.949609
-10	4.120259	4.120068
-5	7.730976	7.732018
0	12.835914	12.836162
5	18.886564	18.886957
10	25.328800	25.329797

TABLE V

$N_R = 4$, $N_T = 12$

SNR (dB)	Capacity (Monte Carlo) (bits/s/Hz)	Capacity (Numerical) (bits/s/Hz)
-15	2.171655	2.172626
-10	4.576217	4.574792
-5	8.530615	8.530668
0	13.934214	13.933461
5	20.122317	20.121336
10	26.612371	26.613163

To further validate the capacity results with CSIT as shown in Fig. 1 (or Fig. 2), we focus on the extreme SNR regimes.

- In the *high* SNR regime, the optimal waterfilling scheme allocates nearly same power for *all* states i.e. $P(\lambda) \approx P/m$ [2, pp. 346-348]. Thus, at high SNR,

$$C = m\,\mathbb{E}_{\boldsymbol{\lambda}}\big[\log(1+\boldsymbol{\lambda}P(\boldsymbol{\lambda}))\big] \approx m\int_0^\infty \log\left(1+\lambda P/m\right) f_{\boldsymbol{\lambda}}(\lambda)d\lambda. \tag{11}$$

  Comparing (11) with (7), it is straightforward that, at high SNR,

$$C \approx \widehat{C} \tag{12}$$

  whenever $m = N_T$. This fact, clearly visible in Fig. 1 at high SNRs, validates the correctness of the capacity values with CSIT presented in this note.
- In the *low* SNR regime, [4] showed that the ergodic capacity with CSIT of this MIMO fading channel scales asymptotically[6] as SNR $\log(1/\text{SNR})$; in particular, an on-off transmission scheme on the strongest eigenmode[7] (say $\boldsymbol{\lambda_{max}}$) is proposed that is "asymptotically (at low SNR) capacity-achieving". This observation is also hinted in [2, Eq. (7.15)]. The ergodic rate achievable with the on-off transmission scheme is given by [4]

$$R = \mathbb{E}_{\boldsymbol{\lambda_{max}}}\big[\log(1+\lambda_{max}P(\lambda_{max}))\big] = \int_\tau^\infty \log\left(1+\lambda P_0\right) f_{\boldsymbol{\lambda_{max}}}(\lambda)d\lambda \tag{13}$$

  where τ is the threshold (chosen same as the *waterfilling* threshold λ_0) and $P_0 = P/\int_\tau^\infty f_{\boldsymbol{\lambda_{max}}}(\lambda)d\lambda$. These rates are obtained numerically for a wide range of low SNR values (see Table XV-Table XIX in Appendix B) and

[4] 10^6 samples are considered for Monte Carlo simulations.

[5] SNR is taken as $P/(mN_0)$, similar to as Eq. (34) in [1].

[6] P/N_0 is taken as SNR in [4].

[7] The CDF of $\boldsymbol{\lambda_{max}}$ is borrowed from [5, Corollary 2]. Alternatively, the PDF of $\boldsymbol{\lambda_{max}}$ is available in [6, Eq. (38)].

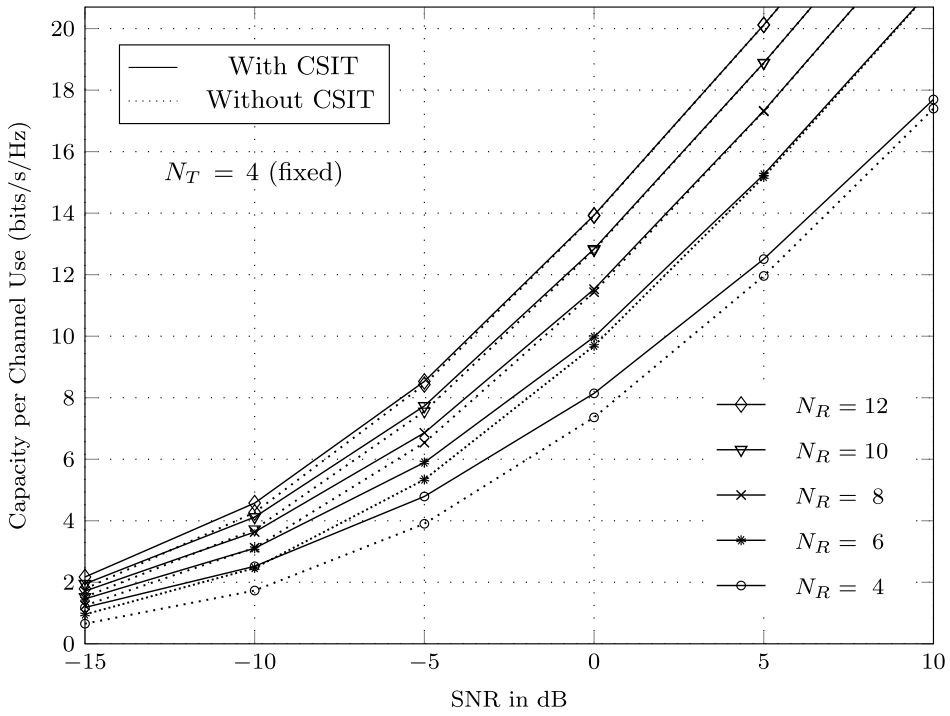

Fig. 1. Ergodic capacity of *coherent* $N_R \times N_T$ MIMO IID Rayleigh channel with $N_T = 4$ (fixed).

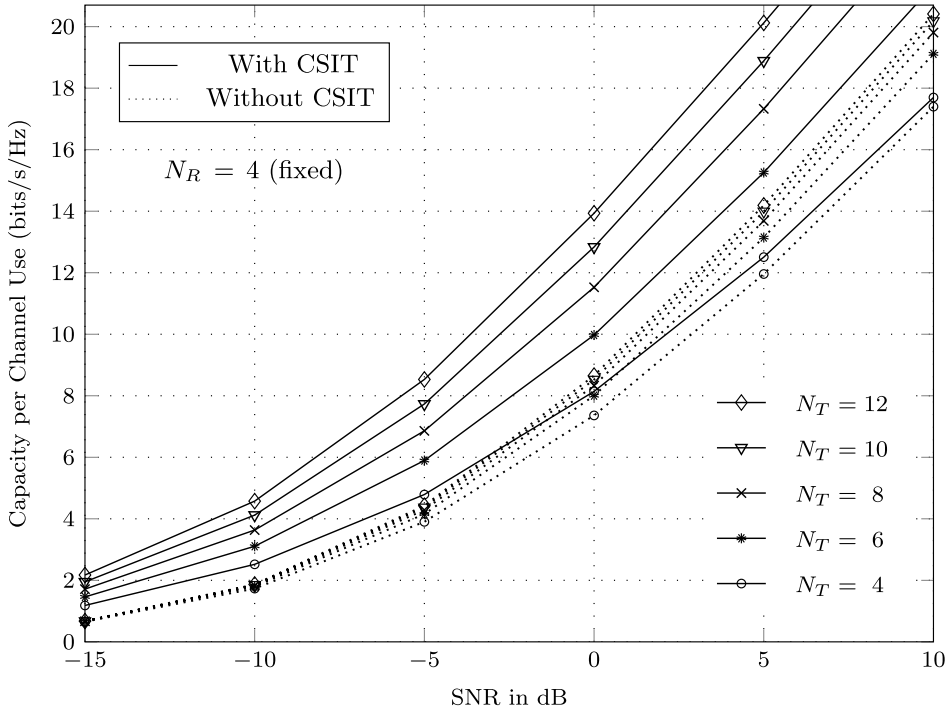

Fig. 2. Ergodic capacity of *coherent* $N_R \times N_T$ MIMO IID Rayleigh channel with $N_R = 4$ (fixed).

plotted in Fig. 3 along with corresponding ergodic capacity with CSIT achieved using the 'optimal' waterfilling scheme over all the non-zero eigenvalues. The ergodic rates achievable using on-off power scheme are close to the computed capacity values with CSIT at sufficiently low SNRs; for example, observe the rates in Fig. 3 at the SNR of -15 dB or lower (for exact comparison, see Table XV-Table XIX in Appendix B). This further validates the correctness of the capacity results with CSIT presented here.

A close examination of the ergodic capacity versus SNR curves in Figs. 5 and 6 in [1], when compared with Figs. 1 and 2 respectively in this note, indicates several differences as follows:

Software used to generate the numerical results and Monte Carlo simulation results in this paper can be downloaded from GitHub: https://github.com/kamalsinghsnu/CapacityOfRayleighFadingMIMOchannel

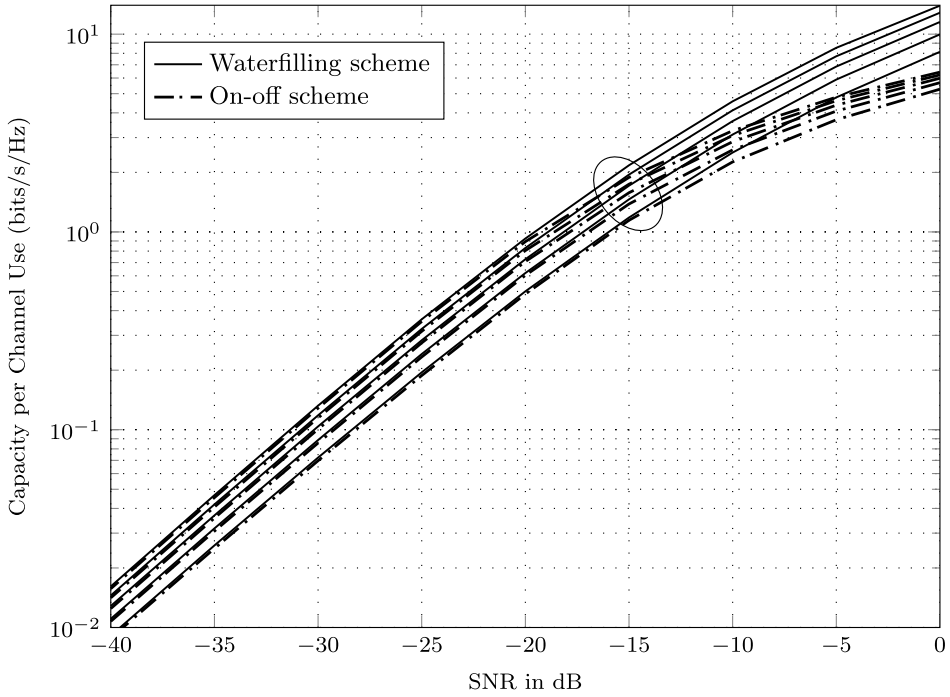

Fig. 3. Ergodic rates of *coherent* $N_R \times N_T$ MIMO IID Rayleigh channel with CSIT and $N_R = 4$ (fixed) at *low* SNRs. For each power scheme (On-off or Waterfilling), the curves correspond, in ascending order, to $N_T = 4, 6, 8, 10, 12$.

- At low SNRs, the capacity values with CSIT in Fig. 5 in [1] show significantly 'larger' improvements with increasing N_R receive antennas than the corresponding values in Fig. 1 in this note. For example, at low enough SNR of -15 dB, the capacity with CSIT in Fig. 5 in [1] varies roughly from around 1 to 5 bits/s/Hz as N_R receive antennas increase from 4 to 12 respectively while the corresponding capacity values for these settings in Fig. 1 (or Fig. 3) in this note range nearly from 1.18 to 2.17 bits/s/Hz respectively.
- Though less noticeable, at high SNRs, the capacity values with CSIT in Fig. 5 in [1] are slightly lower in comparison to the corresponding values in Fig. 1 here.
- Furthermore, the capacity curves *without* CSIT in Figs. 5 and 6 in [1] are inaccurate; for example, the $C \approx \widehat{C}$ approximation at high SNR whenever $m = N_T$ (as noted in Eq. (12)), is missing in Fig. 5 in [1]. Similar discrepancy can be noticed in Fig. 6 in [1] by comparing capacity values of the 4×4 Rayleigh channel with and without CSIT at high SNRs (Eq. (12) holds for this specific channel setting, but is missing in Fig. 6 in [1] as well).

To summarize, there are serious inaccuracies in the ergodic capacity plots (both CSIT and no CSIT) presented in Figs. 5 and 6 in [1], thus resulting in unwarranted comparison and conclusion. These plots are corrected in this note and presented as Figs. 1 and 2 along with detailed justifications.

Fig. 4 in this note is a corrected version of Fig. 8 in [1]. On comparing the capacity values in these figures, the discrepancies can be noticed at large 'minimum number of antennas m' for high SNR values. It is difficult to identify all the sources of numerical errors in the ergodic capacity plots in [1]. One error source is the discrepancy in the threshold value computed in [1]. Eq. (36) in [1] is reproduced below:

$$\int_{\gamma_0}^{\infty} \left(\frac{1}{\gamma_0} - \frac{1}{\gamma}\right) f_{\boldsymbol{\gamma}}(\gamma)\, d\gamma = 1. \tag{14}$$

Eq. (14) is a modification of Eq. (4) with the substitution $\gamma = \lambda \frac{P}{mN_0}$ mentioned in the third footnote. In [1], this cut-off γ_0 is computed and plotted in Fig. 4 for $m = 4$ (fixed), $n = 4, 6, 8, 10$ and SNR (in dB scale) $= -10, -5, 0, 5, 10, \ldots, 40$. For these exact channel settings, we compute the cut-off γ_0 and plotted the values in Fig. 5 in this note. On comparing these two figures, we conclude that the cut-off values for the selected SNR range in [1] are lower than the corresponding cut-off values in Fig. 5 in this note. The error gap (or discrepancy) is significantly larger at low SNR and narrows down at high SNR.

Remark 1: In [1], Section III is devoted to ergodic capacity evaluation for the single receiver antenna systems i.e. $N_R = 1$. The γ_0 plots (Fig. 1) and the capacity curves (both CSIT and no CSIT) (Fig. 2) in [1] for the rank-one channel are 'correct'. Also, the ergodic rates in Fig. 3 in [1] are correct.

In [1], Figs. 9 and 10 are plots of the proposed upper bounds (Eq. (64) and Eq. (66)) on the outage probability, respectively. The outage probability is given by $P_{\text{out}}^{n,m} := F_{\boldsymbol{\lambda_{max}}}(\lambda_0)$ where $F_{\boldsymbol{\lambda_{max}}}(\cdot)$ denotes the CDF of the strongest eigenmode $\boldsymbol{\lambda_{max}}$. For the ease of reading, we reproduce these bounds:

$$P_{\text{out}}^{n,m} \leq \frac{1}{\Gamma(n)\Gamma(m)}[\Gamma(n+m-1) - \Gamma(n+m-1, \lambda_0)] \equiv p_1, \tag{15}$$

$$P_{\text{out}}^{m,m} \leq \min\{p_1,\ p_2\}, \tag{16}$$

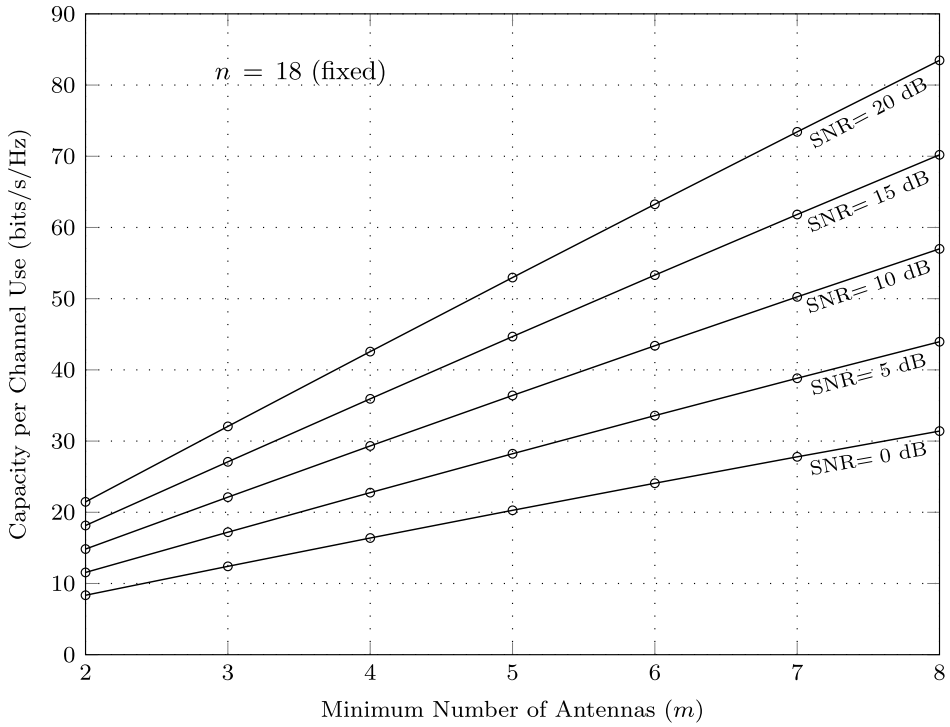

Fig. 4. Ergodic capacity versus minimum number of antennas (m) with $n = 18$ (fixed).

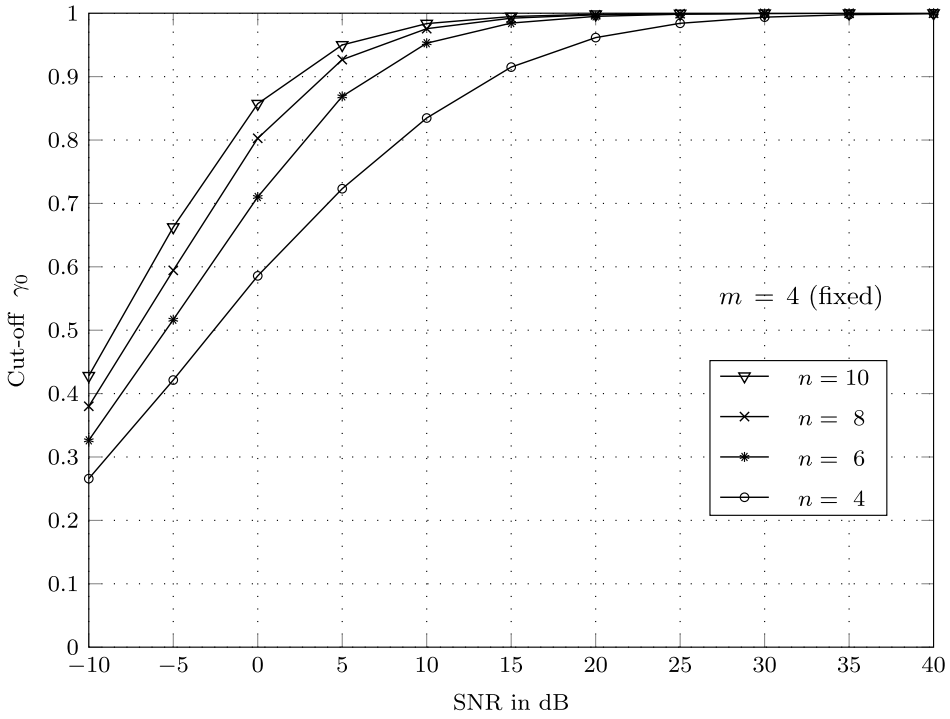

Fig. 5. Optimal cut-off versus SNR for $m = 4$.

where $p_2 \equiv 1 - e^{-m\lambda_0}$. These bounds are evaluated incorrectly in [1] due to errors in the cut-off values; the cut-off γ_0 and the waterfilling threshold λ_0 are related as $\gamma_0 = \frac{P}{m}\lambda_0$ (Eq. (17) in [1]). Figs. 6 and 7 presented in this note are corrected versions of the Figs. 9 and 10, respectively, in [1]. Rather, the outage probability can be computed directly using the $F_{\boldsymbol{\lambda_{max}}}(\cdot)$ distribution function [5, Corollary 2]. For the sake of completeness, we compare the upper bounds in Eq. (15) and Eq. (16) with the actual outage probability in Figs. 8 and 9 respectively in this note.

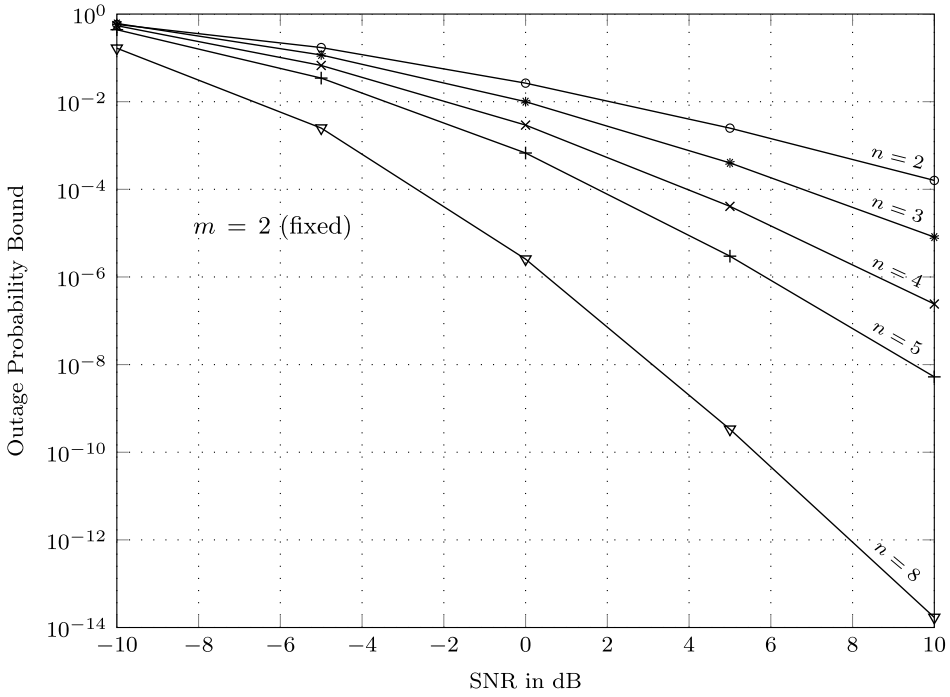

Fig. 6. Upper bound (Eq. (15)) for outage probability of a coherent MIMO IID Rayleigh channel with CSIT and $m = 2$ (fixed). This figure is a corrected version of Fig. 9 in [1].

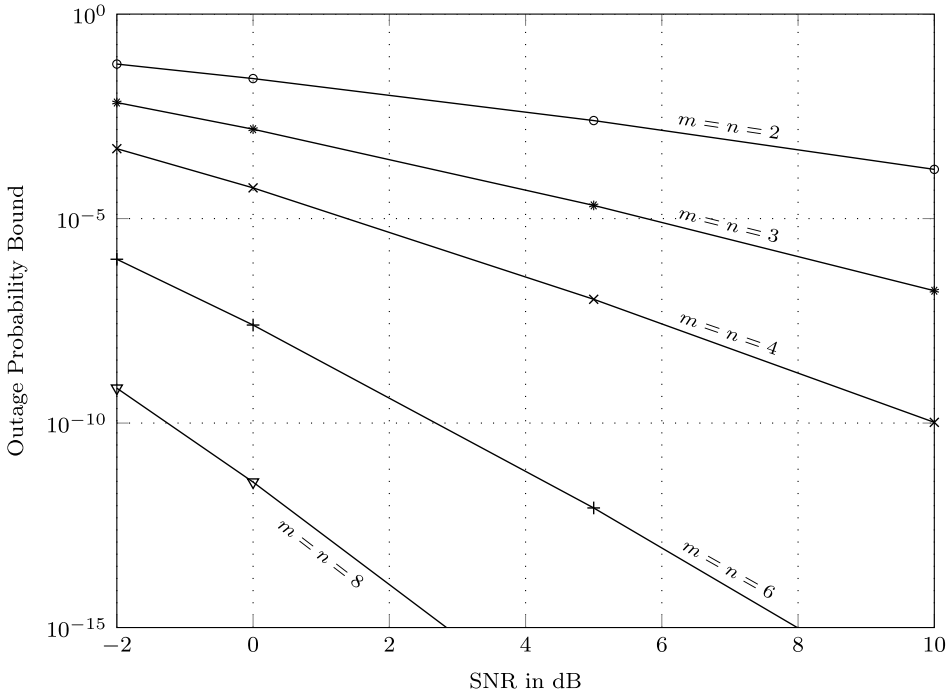

Fig. 7. Upper bound (Eq. (16)) for outage probability of a coherent MIMO IID Rayleigh channel with CSIT and $m = n$. This figure is a corrected version of Fig. 10 in [1].

III. Discussion

An interesting contrast between performances of the coherent MIMO systems with and without CSIT can be inferred from the corrected capacity curves in Figs. 1 and 2:

- For the case when the number of receive antennas N_R is kept fixed and number of transmit antennas N_T is increasing (above N_R), the capacity curves without CSIT suggest the effect of varying N_T is marginal. To justify this, notice that the transmit power is spread out equally across all directions in the $\mathcal{C}^{N_T}$ vector space due to the lack of CSIT, leading to 'wasted' energy which increases with increasing N_T. On the contrary, the diversity gains possible to the receiver improve due to increasing N_T.

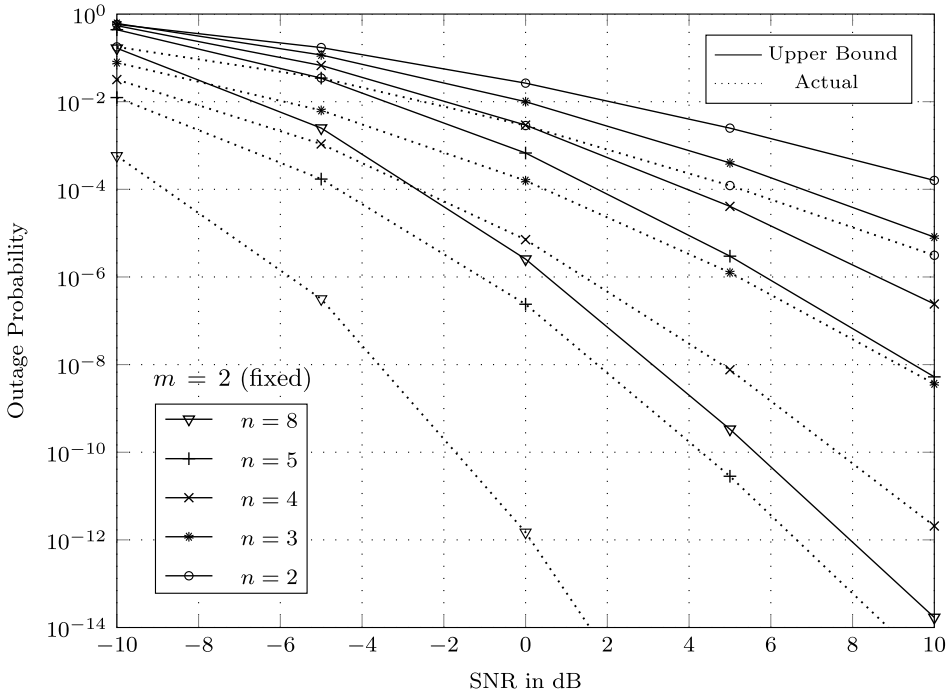

Fig. 8. Upper bound (Eq. (15)) compared with actual outage probability of a coherent MIMO IID Rayleigh channel with CSIT and $m = 2$ (fixed).

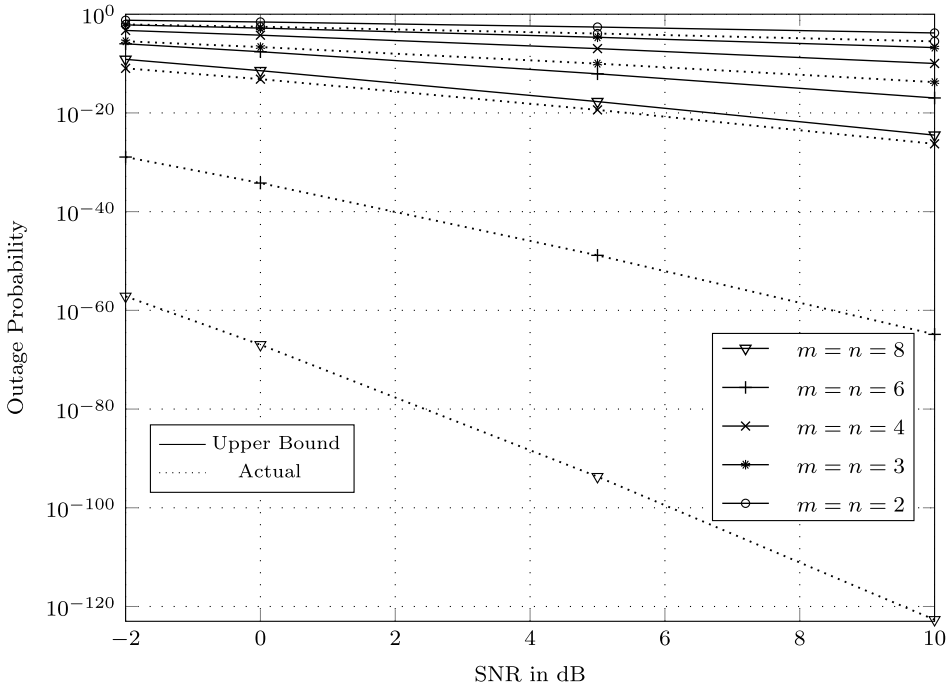

Fig. 9. Upper bound (Eq. (16)) compared with actual outage probability of a coherent MIMO IID Rayleigh channel with CSIT and $m = n$.

Overall, the improvement in the capacity without CSIT is marginal; with CSIT, the vector is projected on only the desirable m non-zero eigenvalues or directions.

- In contrast, for the case when N_T is fixed and N_R is increasing (above N_T), the gap between the capacity curves with CSIT and without CSIT is generally small and nearly vanishes at high SNR (see Eq. (12)). At high SNRs, and since $m = N_T$ holds here, it is easy to deduce that the optimal power allocations at the transmit antennas in both situations (CSIT and no CSIT) are nearly identical. Furthermore, with focus on the capacity without CSIT here, notice that the spread of transmit power or energy across all directions in $\mathcal{C}^{N_T}$ remains 'same' (since N_T is fixed) while the *coherent* receiver is able to exploit higher diversity gains possible due to increasing N_R.

This overall contrast is somewhat limited in [1] because of flaws in the capacity curves.

TABLE VI

$N_R = 4$, $N_T = 4$

SNR (dB)	Capacity (Monte Carlo) (bits/s/Hz)	Capacity (Numerical) (bits/s/Hz)
-15	0.653249	0.653210
-10	1.731278	1.731566
-5	3.901254	3.901646
0	7.360472	7.360570
5	11.954841	11.958356
10	17.402147	17.398369

TABLE VII

$N_R = 4$, $N_T = 6$

SNR (dB)	Capacity (Monte Carlo) (bits/s/Hz)	Capacity (Numerical) (bits/s/Hz)
-15	0.664150	0.664113
-10	1.796232	1.796320
-5	4.152699	4.153194
0	8.004090	8.003924
5	13.143525	13.143428
10	19.114700	19.114446

TABLE VIII

$N_R = 4$, $N_T = 8$

SNR (dB)	Capacity (Monte Carlo) (bits/s/Hz)	Capacity (Numerical) (bits/s/Hz)
-15	0.669718	0.669736
-10	1.830347	1.830585
-5	4.287120	4.287054
0	8.331369	8.330539
5	13.683868	13.685661
10	19.806269	19.806603

TABLE IX

$N_R = 4$, $N_T = 10$

SNR (dB)	Capacity (Monte Carlo) (bits/s/Hz)	Capacity (Numerical) (bits/s/Hz)
-15	0.673125	0.673167
-10	1.851860	1.851785
-5	4.369483	4.369846
0	8.525321	8.525929
5	13.991696	13.992216
10	20.179583	20.179123

TABLE X

$N_R = 4$, $N_T = 12$

SNR (dB)	Capacity (Monte Carlo) (bits/s/Hz)	Capacity (Numerical) (bits/s/Hz)
-15	0.675493	0.675479
-10	1.866260	1.866194
-5	4.426025	4.426032
0	8.655543	8.655479
5	14.188157	14.188736
10	20.413271	20.412153

TABLE XI

$N_R = 6$, $N_T = 4$

SNR (dB)	Capacity (Monte Carlo) (bits/s/Hz)	Capacity (Numerical) (bits/s/Hz)
-15	0.956394	0.956307
-10	2.462461	2.462844
-5	5.339700	5.340373
0	9.687900	9.688512
5	15.175786	15.175911
10	21.334315	21.332693

The implications of these observations for the coherent MIMO system design can be briefly summarized as follows:

TABLE XII

$N_R = 8$, $N_T = 4$

SNR (dB)	Capacity (Monte Carlo) (bits/s/Hz)	Capacity (Numerical) (bits/s/Hz)
-15	1.245405	1.245477
-10	3.122625	3.123057
-5	6.537848	6.537777
0	11.433137	11.432010
5	17.310972	17.311652
10	23.673682	23.672450

TABLE XIII

$N_R = 10$, $N_T = 4$

SNR (dB)	Capacity (Monte Carlo) (bits/s/Hz)	Capacity (Numerical) (bits/s/Hz)
-15	1.521897	1.521850
-10	3.722394	3.723170
-5	7.553039	7.552851
0	12.800568	12.799501
5	18.881360	18.882073
10	25.330437	25.329254

TABLE XIV

$N_R = 12$, $N_T = 4$

SNR (dB)	Capacity (Monte Carlo) (bits/s/Hz)	Capacity (Numerical) (bits/s/Hz)
-15	1.786068	1.786435
-10	4.272003	4.272138
-5	8.429043	8.428782
0	13.916139	13.916232
5	20.120091	20.119217
10	26.612370	26.612935

TABLE XV

$N_R = 4$, $N_T = 4$

SNR (dB)	Capacity (Waterfilling) (bits/s/Hz)	On-off (Monte-carlo) (bits/s/Hz)	On-off (numerical) (bits/s/Hz)
0	8.141455	5.270533	5.264009331
-5	4.788881	3.691180	3.684889873
-10	2.519896	2.259619	2.254272476
-15	1.182636	1.145351	1.141753736
-20	0.500745	0.485424	0.483608496
-25	0.195009	0.187945	0.187270682
-30	0.072300	0.069711	0.069370405
-35	0.025994	0.025088	0.024979542
-40	0.009099	0.008847	0.008820817

TABLE XVI

$N_R = 4$, $N_T = 6$

SNR (dB)	Capacity (Waterfilling) (bits/s/Hz)	On-off (Monte-carlo) (bits/s/Hz)	On-off (numerical) (bits/s/Hz)
0	9.974868	5.683648	5.677020344
-5	5.894041	4.083595	4.077349245
-10	3.107786	2.599575	2.593966946
-15	1.461355	1.384511	1.380272409
-20	0.619716	0.603249	0.600875364
-25	0.241313	0.233272	0.232197311
-30	0.088662	0.085671	0.085386323
-35	0.031695	0.030700	0.030499115
-40	0.011062	0.010743	0.010684742

1) the loss of capacity due to lack of channel state information at the transmitter side for the MIMO Rayleigh fading channel can be made significantly smaller at *medium to high* SNRs by providing a 'larger' antenna array at the receiver.[8]
2) On the other hand, larger antenna array at the transmitter yields minimal improvement in the capacity for the

[8]number of receive antennas to be larger than that of transmit antennas

TABLE XVII

$N_R = 4$, $N_T = 8$

SNR (dB)	Capacity (Waterfilling) (bits/s/Hz)	On-off (Monte-carlo) (bits/s/Hz)	On-off (numerical) (bits/s/Hz)
0	11.527083	5.985882	5.979340923
-5	6.859201	4.374472	4.368011005
-10	3.633938	2.859162	2.853247814
-15	1.714000	1.578669	1.574165663
-20	0.727666	0.708751	0.706173821
-25	0.283272	0.274775	0.273769589
-30	0.103875	0.100618	0.100242818
-35	0.036873	0.035746	0.035616903
-40	0.012848	0.012466	0.012410698

TABLE XVIII

$N_R = 4$, $N_T = 10$

SNR (dB)	Capacity (Waterfilling) (bits/s/Hz)	On-off (Monte-carlo) (bits/s/Hz)	On-off (numerical) (bits/s/Hz)
0	12.836196	6.226041	6.219488459
-5	7.731536	4.606987	4.600511855
-10	4.119671	3.070413	3.064576730
-15	1.949462	1.743438	1.738625987
-20	0.829473	0.805049	0.802063549
-25	0.323232	0.314441	0.313158002
-30	0.118232	0.114694	0.114363686
-35	0.041907	0.040672	0.040480673
-40	0.014515	0.014124	0.014049351

TABLE XIX

$N_R = 4$, $N_T = 12$

SNR (dB)	Capacity (Waterfilling) (bits/s/Hz)	On-off (Monte-carlo) (bits/s/Hz)	On-off (numerical) (bits/s/Hz)
0	13.933972	6.426369	6.419435968
-5	8.531219	4.801641	4.795005000
-10	4.574472	3.249739	3.243676350
-15	2.172983	1.887175	1.882104161
-20	0.925992	0.893189	0.890072923
-25	0.361619	0.352384	0.350926130
-30	0.132287	0.128491	0.127962447
-35	0.046683	0.045373	0.045165040
-40	0.016133	0.015711	0.015626368

lack of CSIT. Alternatively, when the antenna array at the transmitter side is larger than at the receiver end, it is imperative to provide channel information at the transmitter to increase the throughput significantly.

APPENDIX A
ERGODIC CAPACITY (WITHOUT CSIT)

See Tables VI–XIV

APPENDIX B
ERGODIC RATES WITH CSIT (ON-OFF & WATERFILLING POWER SCHEME)

See Tables XV–XIX

REFERENCES

[1] S. K. Jayaweera and H. V. Poor, "Capacity of multiple-antenna systems with both receiver and transmitter channel state information," *IEEE Trans. Inf. Theory*, vol. 49, no. 10, pp. 2697–2709, Oct. 2003.

[2] D. Tse and P. Viswanath, *Fundamentals of Wireless Communication*. Cambridge, U.K.: Cambridge Univ. Press, 2005.

[3] E. Telatar, "Capacity of multi-antenna Gaussian channels," *Eur. Trans. Telecommun.*, vol. 10, no. 6, pp. 585–595, Nov. 1999.

[4] A. Tall, Z. Rezki, and M.-S. Alouini, "MIMO channel capacity with full CSI at low SNR," *IEEE Wireless Commun. Lett.*, vol. 1, no. 5, pp. 488–491, Oct. 2012.

[5] M. Kang and M. Alouini, "Largest eigenvalue of complex Wishart matrices and performance analysis of MIMO MRC systems," *IEEE J. Sel. Areas Commun.*, vol. 21, no. 3, pp. 418–426, Apr. 2003.

[6] A. Zanella, M. Chiani, and M. Z. Win, "On the marginal distribution of the eigenvalues of Wishart matrices," *IEEE Trans. Commun.*, vol. 57, no. 4, pp. 1050–1060, Apr. 2009.

Kamal Singh received the B.Tech. degree in electronics and communication engineering from the National Institute of Technology, Hamirpur, India, in 2003, the M.Tech. degree in telecommunication systems engineering from the Indian Institute of Technology Kharagpur, Kharagpur, India, in 2009, and the Ph.D. degree in electrical engineering from the Indian Institute of Technology Bombay, Mumbai, India, in 2019. From September 2003 to October 2006, he worked as a Senior Engineer with Himachal Futuristic Communications Ltd. (Wireless Division), India. He joined the Department of Electrical Engineering, Shiv Nadar University, India, as an Assistant Professor, in September 2019. His research interests include wireless communications and digital communication simulations.

Chandradeep Singh received the B.E. degree in electronics and communication engineering from Panjab University, India, in 2010, the M.Tech. degree in signal processing from Delhi Technological University, New Delhi, India, in 2012, and the Ph.D. degree in electrical engineering from the Indian Institute of Technology, Bombay, India, in 2020. He is currently a Post-Doctoral Fellow at Department of Electrical Engineering, National Cheng Kung University, Taiwan. His research interests are in wireless networks, cooperative communication and intelligent reflecting surface assisted millimeter wave communication systems.